

UNIVERSIDADE ESTADUAL DE CAMPINAS
SISTEMA DE BIBLIOTECAS DA UNICAMP
REPOSITÓRIO DA PRODUÇÃO CIENTÍFICA E INTELECTUAL DA UNICAMP

Versão do arquivo anexado / Version of attached file:

Versão do Editor / Published Version

Mais informações no site da editora / Further information on publisher's website:

<https://aip.scitation.org/doi/10.1063/1.4746773>

DOI: 10.1063/1.4746773

Direitos autorais / Publisher's copyright statement:

©2012 by AIP Publishing. All rights reserved.

DIRETORIA DE TRATAMENTO DA INFORMAÇÃO

Cidade Universitária Zeferino Vaz Barão Geraldo

CEP 13083-970 – Campinas SP

Fone: (19) 3521-6493

<http://www.repositorio.unicamp.br>

General derivation of the Green's functions for the atomic approach of the Anderson model: application to a single electron transistor (SET)

M. E. Foglio,^{1,a} T. Lobo,² and M. S. Figueira³

¹*Instituto de Física Gleb Wataghin, Universidade Estadual de Campinas, Barão Geraldo 13083-970 Campinas-SP, Brazil*

²*Instituto Federal de Educação, Ciência e Tecnologia do Rio de Janeiro (IFRJ) Campus São Gonçalo, Rua Dr. José Augusto Pereira dos Santos, s/n, Neves - 24425-005 São Gonçalo RJ, CIEP 436 Neusa Brizola, Brazil*

³*Instituto de Física, Universidade Federal Fluminense, Av. Litorânea s/n, 24210-340 Niterói-RJ, Brazil*

(Received 11 September 2011; accepted 31 July 2012; published online 10 August 2012)

We consider the cumulant expansion of the periodic Anderson model (PAM) in the case of a finite electronic correlation U , employing the hybridization as perturbation, and obtain a formal expression of the exact one-electron Green's function (GF). This expression contains effective cumulants that are as difficult to calculate as the original GF, and the atomic approach consists in substituting the effective cumulants by the ones that correspond to the atomic case, namely by taking a conduction band of zeroth width and local hybridization. In a previous work (T. Lobo, M. S. Figueira, and M. E. Foglio, *Nanotechnology* **21**, 274007 (2010)) we developed the atomic approach by considering only one variational parameter that is used to adjust the correct height of the Kondo peak by imposing the satisfaction of the Friedel sum rule. To obtain the correct width of the Kondo peak in the present work, we consider an additional variational parameter that guarantees this quantity. The two constraints now imposed on the formalism are the satisfaction of the Friedel sum rule and the correct Kondo temperature. In the first part of the work, we present a general derivation of the method for the single impurity Anderson model (SIAM), and we calculate several density of states representative of the Kondo regime for finite correlation U , including the symmetrical case. In the second part, we apply the method to study the electronic transport through a quantum dot (QD) embedded in a quantum wire (QW), which is realized experimentally by a single electron transistor (SET). We calculate the conductance of the SET and obtain a good agreement with available experimental and theoretical results. Copyright 2012 Author(s). This article is distributed under a Creative Commons Attribution 3.0 Unported License. [<http://dx.doi.org/10.1063/1.4746773>]

I. INTRODUCTION

The Kondo effect¹ was first observed in metallic matrices with a few percent of dissolved magnetic impurities, like cobalt impurities in gold or cerium impurities in silver. As the temperature is lowered and approaches $T \rightarrow 0K$, the magnetic impurity moment is quenched by the spin-flip scattering of the conduction electrons by the magnetic moment of the impurity. A many-body nonmagnetic ground state singlet is then formed below a characteristic temperature, the Kondo temperature T_K , and the spectral density shows a resonance at the chemical potential: the Kondo peak. This Kondo resonance has low-energy excitations with a characteristic width of $k_B T_K$, where

^aElectronic mail: foglio@ifi.unicamp.br



k_B is the Boltzmann constant, and has been directly observed for a number of dense homogeneous Kondo compounds using high-resolution photoelectron spectroscopy.² The manifestations of the Kondo effect on an atomic length scale have been reported only recently in a single magnetic impurity (adatom) dissolved on a metallic surface substrate, by employing a low-temperature scanning tunneling microscope (STM): first in individual cerium adatoms deposited onto a Ag(111) substrate³ and then in cobalt adatoms deposited onto an Au(111) substrate.⁴ In dense systems it is not possible to control microscopically the Kondo parameters of the lattice or even those of the impurity dissolved in the bulk, but with the advent of nanotechnology the Kondo effect was realized experimentally in quantum dots (QD), with complete control over all of their parameters.^{5,6} The QD systems offers several important advantages in the study of the Kondo effect: the microscopic state of the system is better-defined than in bulk metals and may be even tailored by varying the system's geometry, the important parameters of the system may be precisely measured and tuned, a single impurity site is measured rather than a statistical average over many sites, and finally the local site may be studied out of equilibrium. The Anderson Hamiltonian describes the Kondo effect for the lattice and the impurity: it is composed of strongly correlated f -electrons that are localized, and conduction c -electrons that are considered free. These two types of electrons are subject to the hybridization interaction, that allows their interchange. We have already considered the cumulant expansion of the one-electron Green's function (GF) of the periodic Anderson model (PAM), employing the hybridization as perturbation⁷ (we shall use **I** to indicate Ref. 7). In the present paper we shall derive a formally exact GF, but this expression contains quantities (the effective cumulants) that are difficult to calculate, as much as the original GF. As an approximation we shall replace the exact effective cumulant by those corresponding to an exactly soluble system that is closely related to our problem: we shall use the Anderson model but with all the c -electrons having the same energy (the band has zero width) and a \mathbf{k} independent hybridization (local hybridization). This Anderson Hamiltonian can be exactly diagonalized, and it is possible to calculate analytically its GF and extract an approximate effective cumulant from this GF. This Hamiltonian can be considered as a collection of independent and identical atomic Hamiltonians, one for each site. Each of these single sites can have a maximum of four electrons: two localized electrons and two conduction ones. There are four possible states of f -electrons: the empty state $|0\rangle$, the state $|+\rangle$ with one spin up, the state $|-\rangle$ with one spin down and the state $|d\rangle$ with two local electrons, one for each spin. In a similar way we have four states $|0\rangle, |\uparrow\rangle, |\downarrow\rangle, |\uparrow\downarrow\rangle$ with conduction electrons, so that the dimension of the vector space of states at a given site is sixteen. This atomic Anderson Hamiltonian has then sixteen eigenvalues and eigenstates that we shall call the atomic Anderson solution (AAS), and they give the necessary excitations to generate the Kondo effect. Several authors have studied the AAS solution, and there is a recent review that studies that solution.⁸ We shall employ the AAS as a “seed” for our method,⁹ and shall obtain approximate solutions for both the PAM and the impurity when U is finite.

The atomic approach developed earlier¹⁰ considers only one variational parameter, the position of the conduction atomic level ε_o (cf. Eq. (58)), which is adjusted by imposing the Friedel sum rule to give the correct height of the Kondo peak ($\rho(\mu) = \frac{1}{\pi\Delta}$), but the Kondo temperature, which is related to the width of the Kondo peak, is not reproduced. The atomic approach developed in the present work generalizes the previous one¹⁰ by including an effective hybridization \tilde{V} as an additional variational parameter. This new parameter is adjusted to satisfy the Haldane's Kondo temperature (cf. Eq. (59)) so that the correct width of the Kondo peak is obtained.

The paper is organized as follows: In Section II we present the periodic Anderson model written in terms of Hubbard operators. In Sections III–VI we present the general formalism in terms of the cumulants and the Green's functions, both for the PAM and the single impurity Anderson model (SIAM). In Section VII we introduce the atomic Green's functions and in Section VIII we apply the method to the SIAM. In Sections IX and X we discuss the details of the calculation of the atomic approach with two variational parameters and we present several typical Kondo density of states obtained with the method. In Section XI we apply the method to the calculation of the conductance of the single electron transistor system and we compare the results obtained with available experimental and theoretical results. Finally in Section XII we present the conclusions of the work.¹¹

II. THE MODEL

The PAM is described by the well known Hamiltonian

$$H = \sum_{\mathbf{k},\sigma} E_{\mathbf{k},\sigma} C_{\mathbf{k},\sigma}^\dagger C_{\mathbf{k},\sigma} + \sum_{j,\sigma} E_\sigma f_{j,\sigma}^\dagger f_{j,\sigma} + U \sum_j n_{j,\sigma} n_{j,\bar{\sigma}} + H_h, \quad (1)$$

and the constants and operators in that equation are thoroughly defined in a previous reference⁷ (we shall use **I** to indicate Ref. 7). The fourth term H_h describes the hybridization between the localized and conduction electrons:

$$H_h = \sum_{j,\mathbf{k},\sigma} (V_{j,\mathbf{k},\sigma} f_{j,\sigma}^\dagger C_{\mathbf{k},\sigma} + V_{j,\mathbf{k},\sigma}^* C_{\mathbf{k},\sigma}^\dagger f_{j,\sigma}), \quad (2)$$

with

$$V_{j,\mathbf{k},\sigma} = \frac{1}{\sqrt{N_s}} V_\sigma(\mathbf{k}) \exp(i\mathbf{k} \cdot \mathbf{R}_j). \quad (3)$$

Here we shall employ Hubbard X operators: the $X_{j,ba}$ transforms the state $|a\rangle$ at site j into the state $|b\rangle$ at the same site, where $|a\rangle$ and $|b\rangle$ are eigenstates of the number of electrons. The $X_{j,ba}$ are also discussed in Ref. **I** and are said to be of the Fermi type when $|a\rangle$ and $|b\rangle$ differ by an odd number of Fermions and of the Bose type otherwise. The algebra of these operators is defined by their product rule when they are at the same site:

$$X_{j,ab} \cdot X_{j,cd} = \delta_{b,c} \cdot X_{j,ad}. \quad (4)$$

Employing the X Hubbard operators it is possible to generalize Eq. (2) to the case of several configurations with a rather arbitrary choice of states:

$$H = \sum_{\mathbf{k},\sigma} E_{\mathbf{k},\sigma} C_{\mathbf{k},\sigma}^\dagger C_{\mathbf{k},\sigma} + \sum_{j,a} E_{j,a} X_{j,aa} + H_h = H_0 + H_h, \quad (5)$$

where

$$H_h = \sum_{j,b,a,\mathbf{k},\sigma} \left(V_{j,ba,\mathbf{k},\sigma} X_{j,ba}^\dagger C_{\mathbf{k},\sigma} + V_{j,ba,\mathbf{k},\sigma}^* C_{\mathbf{k},\sigma}^\dagger X_{j,ba} \right). \quad (6)$$

The energies $E_{j,a}$ include all the Coulomb repulsions of the type described by the third term in Eq. (1), and the a and b summations are over all the states $|a\rangle$ and $|b\rangle$ that we want to include in the model: the only restriction is that any hybridization constant must vanish unless state $|a\rangle$ has just one electron more than the state $|b\rangle$.

In the PAM for finite U there are four states $|0\rangle, |+\rangle, |-\rangle, |d\rangle = |+-\rangle$, and it is $f_\sigma = X_{0\sigma} + \sigma X_{\bar{\sigma}d}$. (we write $\sigma = 1$ for $+$ and $\sigma = -1$ for $-$).¹²

To abbreviate, in place of Eq. (6) we write in the interaction picture

$$H_h(\tau) = \sum_{l,l'} V(l,l') Y(l) Y(l'), \quad (7)$$

where

$$Y(l) \equiv Y_\gamma(\tau) = \exp(\tau H_0) Y_\gamma \exp(-\tau H_0) \quad (8)$$

and the subindex γ identifies the operator (cf. after Eq.(3.9) in Ref. **I** for more details).

As we are interested in the Grand Canonical Ensemble of electrons, we should replace the total Hamiltonian H by

$$\mathcal{H} = H - \mu \left\{ \sum_{\mathbf{k},\sigma} C_{\mathbf{k},\sigma}^\dagger C_{\mathbf{k},\sigma} + \sum_{j,a} v_a X_{j,aa} \right\} = \mathcal{H}_0 + H_h, \quad (9)$$

where $X_{j,aa}$ is the occupation number operator of state $|a\rangle$ at site j , and v_a is the number of electrons in that state. This is accomplished by replacing $E_{j,a}$ by

$$\varepsilon_{j,a} = E_{j,a} - \mu v_a \quad (10)$$

for all the ionic states $|a\rangle$ and $E_{\mathbf{k},\sigma}$ by

$$\varepsilon(\mathbf{k}, \sigma) = E_{\mathbf{k},\sigma} - \mu \quad (11)$$

for all the conduction electrons.

III. THE GREEN'S FUNCTIONS IN IMAGINARY FREQUENCY FOR SEVERAL PARTICLES

One can define a general imaginary times Green's Functions (GF)

$$\mathcal{G}(\gamma_1, \tau_1; \dots; \gamma_n, \tau_n) = \left\langle \left(\hat{Y}(\gamma_1, \tau_1) \dots \hat{Y}(\gamma_n, \tau_n) \right)_+ \right\rangle_{\mathcal{H}}, \quad (12)$$

employing the Y_γ operators in the Heisenberg representation

$$\hat{Y}(\gamma, \tau) = \exp(\tau \mathcal{H}) Y_\gamma \exp(-\tau \mathcal{H}) \quad (13)$$

to describe both the Fermi operators $C_{\mathbf{k}\sigma}$ and the Hubbard operators $X_{j,ba}$.

A detailed discussion of these GF is given in Ref. 13 (we shall use II to indicate this reference), and we shall only give here the notation we shall use. For the $X_{j,ba}$ of the Fermi type we set $\gamma = (f; j, \alpha, u)$, with $u = -$, where the index α identifies a transition $|a\rangle \rightarrow |b\rangle$ with the state $|a\rangle$ having just one electron more than $|b\rangle$, and we use $u = +$ to describe the operator $X_{j,ba}^\dagger$ (inverse transition). The site is given by j , the imaginary time in Eq. (13) by τ , and we shall only use f when necessary for clarity. For $C_{\mathbf{k}\sigma}$ we write $\gamma = (c; \mathbf{k}, \sigma, u)$ with $u = -$ and use $u = +$ for $C_{\mathbf{k}\sigma}^\dagger$. We shall also need $X_{j,ba}$ operators where the two states $|a\rangle$ and $|b\rangle$ have equal number of electrons, and we use $u = 1$ for these operators.

One can not employ the usual Feynman type expansions for the GF with X operators, and we shall then use a cumulant expansion⁷ based on the one given by Hubbard^{14,15} for his model. This expansion is discussed in detail in II.

The $V(l, l')$ in Eq. (7) are independent of τ and τ' , and we shall use $v(j, \alpha, \mathbf{k}, \sigma, u)$ in Eq. (6):

$$\begin{aligned} v(j, \alpha, \mathbf{k}, \sigma, +) &= V(f; j, \alpha, +; c; \mathbf{k}, \sigma, -) = V_{j,ba,\mathbf{k},\sigma}, \\ v(j, \alpha, \mathbf{k}, \sigma, -) &= -V(f; j, \alpha, -; c; \mathbf{k}, \sigma, +) = V_{j,ba,\mathbf{k},\sigma}^*. \end{aligned} \quad (14)$$

The explicit site dependence of these coefficients:

$$v(j, \alpha, \mathbf{k}, \sigma, u) = V(\alpha, \mathbf{k}, \sigma, u) N_s^{-\frac{1}{2}} \exp(iu\mathbf{k} \cdot \mathbf{R}_j). \quad (15)$$

is obtained from Eq. (3). The minus sign that should multiply into $V_{j,ba,\mathbf{k},\sigma}^*$, because we anti-commuted two Fermi-type operators from Eq. (6) to obtain Eq. (7), will be absorbed in the rules for the sign of the graph contributions (cf. Appendix C for $\xi = 0$ in I).^{16,17}

The imaginary time Fourier transform of Eq. (12) is discussed in I and II, and is given by

$$\begin{aligned} & \left\langle \left(\hat{Y}(f, \omega; 1) \dots \hat{Y}(f, \omega; r) \hat{Y}(c, \omega; r+1) \dots \hat{Y}(c, \omega; n) \right)_+ \right\rangle_{\mathcal{H}} \\ &= \beta^{-\frac{n}{2}} \int_0^\beta d\tau_1 \dots \int_0^\beta d\tau_n \exp[i(\omega_1 \tau_1 + \dots + \omega_n \tau_n)] \times \\ & \left\langle \left(\hat{Y}(f, \tau; 1) \dots \hat{Y}(f, \tau; r) \hat{Y}(c, \tau; r+1) \dots \hat{Y}(f, \tau; n) \right)_+ \right\rangle_{\mathcal{H}}. \end{aligned} \quad (16)$$

where $\hat{Y}(f, \tau; s) = \hat{Y}(f; j_s, \alpha_s, u_s, \tau_s)$, $\hat{Y}(c, \tau; s) = \hat{Y}(c; \mathbf{k}_s, \sigma_s, u_s, \tau_s)$, and we write ω instead of τ in $\hat{Y}(f, \omega; s)$ and $\hat{Y}(c, \omega; s)$.

When the $\hat{Y}(\gamma_1, \tau_1)$ operators satisfy the necessary relations (cf. Eq.(3.28) in **I**), the frequencies ω_j depend on the type of the Hubbard operator (Bose-like or Fermi-like) and are given by:

$$\omega_j = \frac{\pi v_j}{\beta} \quad \text{where} \quad \begin{cases} v_j = 0, \pm 2, \pm 4 \dots & \text{Bose-like} \\ v_j = 1, \pm 3, \pm 5 \dots & \text{Fermi-like.} \end{cases} \quad (17)$$

The rules for calculating all the diagrams that appear in the diagrammatic expansion are thoroughly discussed in Ref. **II** (cf. Section II A). From the derivation of these rules (cf. Ref. **II**) and the invariance under time translation (i.e. \mathcal{H} does not depend on τ) one can show that unless

$$\omega_1 + \omega_2 + \dots + \omega_n = 0 \quad (18)$$

the GF given in Eq. (16) is zero. Although we shall not consider the transformation of real into imaginary space, we shall notice that because of the invariance under lattice translation (cf. Section II A in **II**), the GF in the reciprocal space and imaginary time also goes to zero unless

$$\mathbf{k}_1 u_1 + \mathbf{k}_2 u_2 + \dots + \mathbf{k}_n u_n = 0, \quad (19)$$

where the $u_s = \pm 1$ takes care of the creation ($u_s = +1$) or destruction ($u_s = -1$) of electrons in the GF, as discussed after Eq. (13).

IV. THE EFFECTIVE CUMULANT

In this work we are interested in the one electron GF of the f-electrons, and in reciprocal space and imaginary frequency we have

$$\begin{aligned} \mathcal{G}^{ff}(\mathbf{k}, \alpha, u, \omega; \mathbf{k}', \alpha', u', \omega') = & \\ \times \frac{1}{\beta N_s} \sum_{j, j'} \exp[i(u\mathbf{k} \cdot \mathbf{R} + u'\mathbf{k}' \cdot \mathbf{R}')] \int_0^\beta d\tau \int_0^\beta d\tau' \exp[i(\omega\tau + \omega'\tau')] & \\ \times \left\langle \left(\hat{Y}(f; j, \alpha, u, \tau) \hat{Y}(f'; j', \alpha', u', \tau') \right)_+ \right\rangle_{\mathcal{H}}, & \end{aligned} \quad (20)$$

where \mathbf{R}' is the position of site j' . In particular we need $\mathcal{G}^{ff}(\mathbf{k}, \alpha, u = -, \omega; \mathbf{k}', \alpha', u' = +, \omega')$, the transform of $\left\langle \left(\hat{X}_{j, \alpha}(\tau_1) \hat{X}_{j', \alpha'}^\dagger(0) \right)_+ \right\rangle_{\mathcal{H}}$, and to abbreviate the notation we employ Eqs. (18) and (19) and the fact that the number of electrons is conserved:

$$\mathcal{G}^{ff}(\mathbf{k}, \alpha, u = -, \omega; \mathbf{k}', \alpha', u', \omega') =$$

$$\mathcal{G}_{\alpha\alpha'}^{ff}(\mathbf{k}, i\omega_j) \Delta(u + u') \Delta(u\mathbf{k} + u'\mathbf{k}') \Delta(\omega_j + \omega'_j), \quad (21)$$

where ω and ω' are given by Eq. (17).¹⁸

Employing Fermi or Bose operators, the f-electron one-particle GF is obtained by a sum of simple diagrams, where the vertices are replaced by the sum of all “proper” (or irreducible) diagrams,^{19,20} and a similar technique has been used when the electron hopping is employed as perturbation.^{21,22} In **I** we employed the hybridization as a perturbation in the cumulant expansion of the PAM, and used the exact solution of the conduction electrons without hybridization as a part of the zeroth order Hamiltonian. We then extended Metzner’s derivation²¹ to the PAM with $U \rightarrow \infty$, showing for our model²³ the validity of the same type of results he obtained, and employing them to derive the GF used in Ref. 24. In the diagrams of our cumulant expansion (cf. **I** and **II**) the vertices are f-electron cumulants (FV) or conduction electron cumulants (CV), joined by edges that correspond to the perturbation. One can then define an effective cumulant $M_{\alpha\alpha'}^{eff}(\mathbf{k}, z_n)$ by taking together all the diagrams of $\mathcal{G}_{\alpha\alpha'}^{ff}(\mathbf{k}, z_n)$ that can not be separated by cutting a single edge (the usual “proper” or “irreducible” diagrams) and use it to rearrange the diagram expansion, as it is usually done with Feynman expansions. The exact GF $\mathcal{G}_{\alpha\alpha'}^{ff}(\mathbf{k}, z_n)$ then corresponds to a simple family of diagrams (cf. Fig 1(a) in Section III of **II** and discussion thereof) and is obtained by replacing all the bare cumulants associated to their FV by the effective cumulants $M_{\alpha\alpha'}^{eff}(\mathbf{k}, z_n)$.

In the case of finite U there are sixteen exact GF, and we rearrange them in a 4×4 matrix. When the spin commutes with the Hamiltonian, this matrix splits into two independent 2×2 matrices, one for each spin component. We call $\mathbf{G}_\sigma^{ff}(\mathbf{k}, z_n)$ each of the two matrices, and do not use the subindex σ unless necessary. The $\mathbf{G}^{ff}(\mathbf{k}, z_n)$ were derived in Appendix D of **II** and expressed in terms of an effective cumulant matrix $\{\mathbf{M}\}_{\alpha\alpha'} = M_{\alpha\alpha'}^{eff}(\mathbf{k}, z)$ (cf. Eq. (D28) in **II** with $u = -$), and in real space the $\mathcal{G}_{\alpha\alpha'}^{ff}(\mathbf{j}, z_n)$ were derived employing an effective cumulant matrix $\{\mathbf{M}\}_{\alpha\alpha'} = M_{\alpha\alpha'}^{eff}(\mathbf{j}, z)$ (cf. Eq. (D52) in **II** with $u = -$). These effective cumulants also split into two independent 2×2 matrices \mathbf{M} . One can extend the derivation in **II** to any number of transitions α , but we shall only consider here the Anderson model for finite U (two transitions $\alpha = (0, \sigma), (\bar{\sigma}, d)$ per spin) and for $U \rightarrow \infty$ (only one transition $\alpha = (0, \sigma)$ per spin).

V. THE EXACT FORMAL GREEN'S FUNCTIONS FOR THE PAM

When we apply the cumulant expansion to $\mathcal{G}_{\alpha\alpha'}^{ff}(\mathbf{k}, z)$ (cf. Eq. (21)), the term with $n + 1$ effective cumulants in the series is (cf. Eq. (D30) in **II**)

$$\{(\mathbf{M} \cdot \mathbf{W})^n \cdot \mathbf{M}\}_{\alpha\alpha'} = \{\mathbf{M} \cdot (\mathbf{W} \cdot \mathbf{M})^n\}_{\alpha\alpha'}, \quad (22)$$

where $\{\mathbf{W}\}_{\alpha'\alpha} \equiv W_{\alpha'\alpha}(\mathbf{k}, \sigma, z)$ with

$$W_{\alpha'\alpha}(\mathbf{k}, \sigma, z) = V^*(\alpha', \mathbf{k}, \sigma) V(\alpha, \mathbf{k}, \sigma) \mathcal{G}_{c,\sigma}^0(\mathbf{k}, z). \quad (23)$$

We have used the GF of the free conduction electron:

$$\mathcal{G}_{c,\sigma}^0(\mathbf{k}, z) = \frac{-1}{z - \varepsilon(\mathbf{k}, \sigma)}, \quad (24)$$

as well as $V(\alpha', \mathbf{k}, \sigma, +) = V(\alpha', \mathbf{k}, \sigma)$ and $V(\alpha, \mathbf{k}, \sigma, -) = V^*(\alpha, \mathbf{k}, \sigma)$ (cf. Eqs. (14) and (15)). We define $\mathbf{A} \equiv (\mathbf{W} \cdot \mathbf{M})$, which gives

$$A_{\alpha\alpha'}(\mathbf{k}, \sigma, z) = \sum_{\alpha_1} W_{\alpha\alpha_1}(\mathbf{k}, \sigma, z) M_{\alpha_1\alpha'}(\mathbf{k}, \sigma, z), \quad (25)$$

and the series of the exact GF then reads

$$\begin{aligned} \mathcal{G}_{\alpha\alpha'}^{ff} &= \{\mathbf{M} + \mathbf{M} \cdot \mathbf{W} \cdot \mathbf{M} + \mathbf{M} \cdot (\mathbf{W} \cdot \mathbf{M})^2 + \dots\}_{\alpha\alpha'} \\ &= \{\mathbf{M} + \mathbf{M} \cdot \mathbf{A} + \mathbf{M} \cdot (\mathbf{A})^2 + \dots\}_{\alpha\alpha'} \\ &= \{\mathbf{M} \cdot (\mathbf{I} + \mathbf{A} + \mathbf{A}^2 + \dots)\}_{\alpha\alpha'}. \end{aligned} \quad (26)$$

It then follows that the components of the matrix $\mathbf{G}^{ff}(\mathbf{k}, \sigma, z)$ are

$$\mathcal{G}_{\alpha\alpha'}^{ff}(\mathbf{k}, \sigma, z) = \{\mathbf{M} \cdot (\mathbf{I} - \mathbf{A})^{-1}\}_{\alpha\alpha'}, \quad (27)$$

and we can write

$$\mathbf{G}^{ff} = \mathbf{M} \cdot (\mathbf{I} - \mathbf{A})^{-1} = \mathbf{M} \cdot (\mathbf{I} - \mathbf{W} \cdot \mathbf{M})^{-1}. \quad (28)$$

From this relation it follows that the matrix of the exact effective cumulant is

$$\mathbf{M} = (\mathbf{I} + \mathbf{G}^{ff} \cdot \mathbf{W})^{-1} \cdot \mathbf{G}^{ff}. \quad (29)$$

The calculation of \mathbf{M} is as difficult as that of the exact GF \mathbf{G}^{ff} , and we shall then use a model that is exactly soluble to obtain the corresponding GF, that we shall then introduce into Eq. (29) to find the corresponding approximate effective cumulant. As the exactly soluble model we shall use the same Anderson model, but with a zeroth-width conduction band and a local hybridization. This model has the advantage that its cumulant expansion has the same graphs of the original model, and we shall call $\mathbf{G}^{ff,at}(z)$ its exact GF. Introducing $\mathbf{G}^{ff,at}(z)$ into Eq. (29) we obtain

$$\mathbf{M}^{at}(z) = (\mathbf{I} + \mathbf{G}^{ff,at}(z) \cdot \mathbf{W})^{-1} \cdot \mathbf{G}^{ff,at}(z), \quad (30)$$

and substituting \mathbf{M} in Eq. (28) by this $\mathbf{M}^{at}(z)$, we obtain our approximate GF for the PAM.

VI. THE EXACT FORMAL GREEN'S FUNCTIONS FOR THE IMPURITY ANDERSON MODEL

For the SIAM we only need the imaginary time Fourier transform (cf. Eq. (20)), and instead of Eq. (21) we have

$$\begin{aligned} \mathcal{G}^{ff}(\mathbf{j}, \alpha, u = -, \omega; \mathbf{j}', \alpha', u', \omega') &= \\ &= \mathcal{G}_{\alpha\alpha'}^{ff}(\mathbf{j}, i\omega) \Delta(u + u') \Delta(\omega + \omega') \delta(\mathbf{j}, \mathbf{j}'), \end{aligned} \quad (31)$$

where we have introduced $\mathcal{G}_{\alpha\alpha'}^{ff}(\mathbf{j}, i\omega)$. The derivation in this case follows the same steps employed in the previous section. The term that has $n + 1$ effective cumulants in the expansion of $\mathcal{G}_{\alpha\alpha'}^{ff}(\mathbf{j}_i, z)$ is again (cf. Eq. (D54) in II)

$$\{(\mathbf{M} \cdot \mathbf{W})^n \cdot \mathbf{M}\}_{\alpha\alpha'} = \{\mathbf{M} \cdot (\mathbf{W} \cdot \mathbf{M})^n\}_{\alpha\alpha'},$$

where

$$\{\mathbf{M}\}_{\alpha,\alpha'} = M_{\alpha\alpha'}^{eff}(\mathbf{j}_i, z_n, u), \quad (32)$$

(cf. Eq. (D52) in II) and

$$\begin{aligned} \{\mathbf{W}\}_{\alpha',\alpha} &= W_{\alpha',\alpha}(\sigma, z_n) = \\ &= (1/N_s) \sum_{\mathbf{k}} V^*(\alpha', \mathbf{k}, \sigma) V(\alpha, \mathbf{k}, \sigma) \mathcal{G}_{c,\sigma}^0(\mathbf{k}, z_n), \end{aligned} \quad (33)$$

(cf. Eqs. (D50,D53) in II). The components $\mathcal{G}_{\alpha\alpha'}^{ff}(\mathbf{j}_i, z_n)$ of the exact formal solution then give the GF matrix

$$\mathbf{G}^{ff} = \mathbf{M} \cdot (\mathbf{I} - \mathbf{W} \cdot \mathbf{M})^{-1}, \quad (34)$$

so that again

$$\mathbf{M} = (\mathbf{I} + \mathbf{G}^{ff} \cdot \mathbf{W})^{-1} \cdot \mathbf{G}^{ff}. \quad (35)$$

Introducing the approximate $\mathbf{G}^{ff,at}(\mathbf{j}_i, z_n) = \mathbf{G}^{ff,at}(z_n)$ into Eq. (35) we find

$$\mathbf{M}^{at}(z_n) = (\mathbf{I} + \mathbf{G}^{ff,at}(z_n) \cdot \mathbf{W})^{-1} \cdot \mathbf{G}^{ff,at}(z_n), \quad (36)$$

and substituting into Eq. (34) we obtain the approximate GF of the SIAM employed in this work.

VII. CALCULATION OF THE ATOMIC GREEN'S FUNCTIONS

The Hamiltonian of the problem, given in Eqs. (5) and (6), can be diagonalized exactly²⁵ when all the conduction electrons have the same energy and the hybridization is independent of \mathbf{k} (i.e. a local hybridization), and it is then possible to calculate the exact GF analytically. When $E_{\mathbf{k},\sigma} = E_0^a$ and $V_{j\alpha,\mathbf{k},\sigma} = V_{j\alpha,\sigma}$ the problem is fully local, and it is convenient to use the Wannier representation for the c-electrons operators $C_{j,\sigma}^\dagger$ and $C_{j,\sigma}$. One can then write $H_r = \sum_j H_j$, where

$$\begin{aligned} H_j &= \sum_{\sigma} E_0^a C_{j,\sigma}^\dagger C_{j,\sigma} + \sum_{a,\sigma} E_{ja} X_{j,aa} \\ &+ \sum_{\alpha,\sigma} \left(V_{j\alpha,\sigma} X_{j,\alpha}^\dagger C_{j\sigma} + V_{j\alpha,\sigma}^* C_{j\sigma}^\dagger X_{j,\alpha} \right), \end{aligned} \quad (37)$$

is a local Hamiltonian, and we can drop the subindex j because the system is uniform. We write $|n, r\rangle$ for an eigenstate of H_j with n electrons in that state and energy $E_{n,r}$, where r identifies the state between all those with the same n . It is convenient to write the eigenvalue equation as

$$\mathcal{H} |n, r\rangle = \varepsilon_{n,r} |n, r\rangle, \quad (38)$$

where $\varepsilon_{n,r} = E_{n,r} - n\mu$ (cf. Eq. (10)), and \mathcal{H} is the single-site equivalent to the Hamiltonian in Eq. (9).

We need the components $\mathcal{G}_{\alpha\alpha'}^{ff,at}(i\omega_s)$ of the matrix $\mathbf{G}^{ff,at}(i\omega_s)$ employed in Eq. (36), which are the Fourier transforms of the approximate GF $\left\langle\left(X_{j,\alpha}(\tau)X_{j,\alpha'}^\dagger(\tau')\right)\right\rangle_{+\mathcal{H}}$ and are given by Eq. (C13) in Ref. II:

$$\left\langle\left(X_{j,\alpha}(\omega_s)X_{j,\alpha'}^\dagger(\omega'_s)\right)\right\rangle_{+\mathcal{H}} = \Delta(\omega_s + \omega'_s) \mathcal{G}_{\alpha\alpha'}^{ff,at}(i\omega_s). \quad (39)$$

These GF have been derived in detail in Section V of II, (cf. also Eq. (A.1) of Ref 10) and are given by

$$\mathcal{G}_{\alpha\alpha'}^{ff,at}(i\omega_s) = -e^{\beta\Omega} \sum_{n,r,r'} \frac{\exp(-\beta\varepsilon_{n-1,r}) + \exp(-\beta\varepsilon_{n,r'})}{i\omega_s + \varepsilon_{n-1,r} - \varepsilon_{n,r'}} \times \\ \langle n-1, r | X_{j,\alpha} | n, r' \rangle \langle n, r' | X_{j,\alpha'}^\dagger | n-1, r \rangle. \quad (40)$$

Equivalent expressions for $\mathcal{G}_{\sigma\sigma'}^{cc,at}(i\omega_s)$, $\mathcal{G}_{\sigma\sigma'}^{fc,at}(i\omega_s)$ and $\mathcal{G}_{\sigma\sigma'}^{cf,at}(i\omega_s)$ can be obtained in the same way. Using these functions as components, we define four matrices $\mathbf{G}^{ff,at}(i\omega_s)$, $\mathbf{G}^{cc,at}(i\omega_s)$, $\mathbf{G}^{fc,at}(i\omega_s)$ and $\mathbf{G}^{cf,at}(i\omega_s)$, and we can include all of them in a single matrix:

$$\mathbf{G}^{at}(i\omega_s) = \begin{bmatrix} \mathbf{G}^{ff,at}(i\omega_s) & \mathbf{G}^{fc,at}(i\omega_s) \\ \mathbf{G}^{cf,at}(i\omega_s) & \mathbf{G}^{cc,at}(i\omega_s) \end{bmatrix}. \quad (41)$$

The matrix $\mathbf{G}^{at}(i\omega_s)$ is 6×6 for finite U and is 4×4 for infinite U .

VIII. DETAILED CALCULATION OF THE APPROXIMATE GF

Employing Eqs. (14) and (15) as well as Eq. (D.16) from II, we shall rewrite the constant $V_{j,\alpha,\mathbf{k},\sigma}$ of the Hamiltonian H_h that describes the hybridization as follows:

$$V_{j,\alpha,\mathbf{k},\sigma} = V(\alpha, \mathbf{k}, \sigma) N_s^{-\frac{1}{2}} \exp(iu\mathbf{k} \cdot \mathbf{R}_j). \quad (42)$$

In the SIAM there are just four local states $|0\rangle$, $|+\rangle$, $|-\rangle$ and $|d\rangle = |+, -\rangle$, so that there are only four X operators destroying one electron at the impurity site. To distinguish between these X operators we shall use indexes $I_x = 1, 2, 3, 4$ (cf. Table 1 of our earlier work¹⁰), corresponding respectively to the following transitions $\alpha = (b, a)$: $(0, +)$, $(0, -)$, $(-, d)$, and $(+, d)$. We then have that $I_x = 1, 3$ correspond to the spin up and $I_x = 2, 4$ to the spin down. The components $\{\mathbf{W}\}_{\alpha',\alpha} = W_{\alpha',\alpha}(\mathbf{k}, \sigma, z_n)$ of the matrix \mathbf{W} for the PAM are given by Eq. (23), while those for the SIAM are given in Eq. (33).

Taking a spin independent hybridization in the Anderson model the coefficients $V(0\sigma, \mathbf{k}, \bar{\sigma})$, $V(\bar{\sigma}d, \mathbf{k}, \bar{\sigma})$, $V(0\bar{\sigma}, \mathbf{k}, \sigma)$ and $V(\sigma d, \mathbf{k}, \sigma)$ vanish, and for local mixing (i.e. \mathbf{k} independent) one obtains

$$V(0\sigma, \mathbf{k}, \sigma) = V, \quad (43)$$

$$V(\bar{\sigma}d, \mathbf{k}, \sigma) = \sigma V, \quad (44)$$

assuming that $V_\sigma(\mathbf{k})$ is independent of $\sigma = \pm 1$. If the Hamiltonian does not depends on spin (cf. Section IV), the 4×4 matrices \mathbf{G}^{ff} , \mathbf{M} , \mathbf{W} and $\mathbf{A} = \mathbf{W} \cdot \mathbf{M}$ take a diagonal form with 2×2 matrices in the diagonal:

$$\mathbf{G}^{ff} = \begin{pmatrix} \mathbf{G}_\uparrow^{ff} & 0 \\ 0 & \mathbf{G}_\downarrow^{ff} \end{pmatrix}. \quad (45)$$

To write Eq. (45) the order of the matrix elements has been changed, so that $I_x = 1, 3$ corresponds to \mathbf{G}_\uparrow^{ff} and $I_x = 2, 4$ to $\mathbf{G}_\downarrow^{ff}$.

Using Eqs. (24), (43), and (44), the following submatrices are obtained for the PAM

$$\mathbf{W}_{\uparrow}(\mathbf{k}, z) = |V|^2 \mathcal{G}_{c,\uparrow}^0(\mathbf{k}, z) \begin{pmatrix} 1 & 1 \\ 1 & 1 \end{pmatrix}, \quad (46)$$

$$\mathbf{W}_{\downarrow}(\mathbf{k}, z) = |V|^2 \mathcal{G}_{c,\downarrow}^0(\mathbf{k}, z) \begin{pmatrix} 1 & -1 \\ -1 & 1 \end{pmatrix}. \quad (47)$$

For the SIAM, when the impurity is at the origin, it is

$$\mathbf{W}_{\uparrow}(z) = |V|^2 \varphi_{\uparrow}(z) \begin{pmatrix} 1 & 1 \\ 1 & 1 \end{pmatrix}, \quad (48)$$

$$\mathbf{W}_{\downarrow}(z) = |V|^2 \varphi_{\downarrow}(z) \begin{pmatrix} 1 & -1 \\ -1 & 1 \end{pmatrix}, \quad (49)$$

and we have

$$\varphi_{\sigma}(z) = \frac{1}{N_s} \sum_{\mathbf{k}} \mathcal{G}_{c,\sigma}^0(\mathbf{k}, z). \quad (50)$$

When we consider a rectangular band in $[A, B]$, with $B = A + 2D$, it is

$$\varphi_{\sigma}(z) = \frac{1}{2D} \ln \left(\frac{z - B + \mu}{z + A + \mu} \right), \quad (51)$$

and the chemical potential μ is present in $\varphi_{\sigma}(z)$ because $\varepsilon(\mathbf{k}, \sigma) = E_{\mathbf{k},\sigma} - \mu$ appears in $\mathcal{G}_{c,\sigma}^0(\mathbf{k}, z)$. The relation

$$\mathbf{G}_{\sigma}^{ff} = \mathbf{M}_{\sigma} \cdot (\mathbf{I} - \mathbf{W}_{\sigma} \mathbf{M}_{\sigma})^{-1}, \quad (52)$$

is valid for the PAM (Eq. (28)) and for the SIAM (Eq. (34)), so in both cases one obtains (cf. Section IV)

$$\mathbf{M}_{\sigma} = (\mathbf{I} + \mathbf{G}_{\sigma}^{ff} \cdot \mathbf{W}_{\sigma})^{-1} \cdot \mathbf{G}_{\sigma}^{ff}. \quad (53)$$

IX. THE ATOMIC APPROACH FOR THE SINGLE IMPURITY ANDERSON MODEL

When we introduce the components m_{IJ} of the exact cumulants we write

$$\mathbf{M}_{\uparrow} = \begin{pmatrix} m_{11} & m_{13} \\ m_{31} & m_{33} \end{pmatrix} \quad ; \quad \mathbf{M}_{\downarrow} = \begin{pmatrix} m_{22} & m_{24} \\ m_{42} & m_{44} \end{pmatrix}. \quad (54)$$

If we then invert analytically the 2×2 matrix in Eq. (52) and use Eqs. (48) and (49) and Eq. (54), we obtain analytic expressions of the exact f electrons GF. They are explicitly given in Eqs. (26) and (27) of Ref. 10, and the corresponding approximate GF are obtained by replacing the exact effective cumulants by the approximate ones. These cumulants were already defined in Eq. (36):

$$\mathbf{M}_{\sigma}^{at} = (\mathbf{I} + \mathbf{G}_{\sigma}^{ff,at} \cdot \mathbf{W}_{\sigma}^o)^{-1} \cdot \mathbf{G}_{\sigma}^{ff,at}, \quad (55)$$

and we should use the atomic solution (AAS) in Eq. (40) to calculate the $G_{\sigma}^{ff,at}(z)$ (cf. appendix of Ref. 10).

Instead of the \mathbf{W} that was employed in the exact formal solution (cf. Eqs. (48) and (49)), we should use the following \mathbf{W}_{σ}^o in Eq. (55):

$$\mathbf{W}_{\uparrow}^o(z) = |\tilde{V}|^2 \varphi_{\uparrow}^o(z) \begin{pmatrix} 1 & 1 \\ 1 & 1 \end{pmatrix}, \quad (56)$$

$$\mathbf{W}_{\downarrow}^o(z) = |\tilde{V}|^2 \varphi_{\downarrow}^o(z) \begin{pmatrix} 1 & -1 \\ -1 & 1 \end{pmatrix}, \quad (57)$$

where

$$\varphi_\sigma^o(z) = \frac{-1}{z - \varepsilon_o}, \quad (58)$$

is the free GF $\mathcal{G}_{c,\sigma}^0(\mathbf{k}, z)$ of the band with zeroth-width at ε_o . The contribution of the c electrons is overestimated, because they are all at the energy level ε_o , and to moderate this effect we use $\tilde{V} = \Delta$ in both the intermediate valence and the magnetic regions, where $\Delta = \pi V^2/2D$ is the Anderson parameter. In the Kondo region, we use the universality of the electric conductance $G(T/T_K)^{26,27}$ to extract the T_K associated to the G that was calculated employing a given value of \tilde{V} in the atomic approach (we give later more details of this procedure), and then vary this parameter so that the Kondo temperature T_K coincides with the usual value (see e.g. Eq. 6.115 in Hewson's book²⁸):

$$k_B T_K = \sqrt{\frac{U\Delta}{2}} \exp\left(\frac{-\pi|\epsilon_f||\epsilon_f + U|}{2U\Delta}\right). \quad (59)$$

In the atomic approach, we substitute the exact effective cumulant M_σ that appears in Eq. (52), by the exact atomic one M_σ^{at} of Eq. (55) after using the conditions given in Eqs. (56)–(59). The corresponding M_σ^{ap} with components m_{IJ}^{ap} are given in Eqs. (39) and (40) of Ref. 10, and the Green's functions in the atomic approach are then obtained by introducing these approximate M_σ^{ap} into Eq. (52).

One should notice that the choice of $\varphi_\sigma^o(z)$ with an adequate parameter ε_o is essential to obtain a correct Kondo's peak height at the chemical potential μ in the atomic approach: if instead we use Eqs. (48)–(51) two or more peaks appear around the chemical potential, as obtained in early works using the atomic solution of the Anderson model.^{8,29–31} At the same time, the choice in the atomic solution of an hybridization \tilde{V} such that the Kondo temperature in Eq. (59) is obtained from the conductance calculated in the atomic approach, is fundamental to guarantee the correct width of the Kondo peak at the chemical potential μ . The formal expressions of the matrices $\mathbf{G}_\sigma^{fc,ap}(\mathbf{j}_i = 0, \mathbf{k}, i\omega)$ and $\mathbf{G}_\sigma^{cf,ap}(\mathbf{k}, \mathbf{j}' = 0, i\omega)$ associated to the cross GF of the impurity, as well as those of the pure conduction electron GF $\mathbf{G}_\sigma^{cc,ap}(\mathbf{k}, \mathbf{k}', i\omega)$, are defined and calculated in reference II, which is an extended electronic version of the present paper, deposited in the Los Angeles repository.¹³ In that reference we also give the GF $\mathbf{G}_\sigma^{fc,ap}(i\omega)$ and the $\mathbf{G}_\sigma^{cf,ap}(i\omega)$ when the conduction electrons are in the Wannier representation, as well as the corresponding $\mathbf{G}_\sigma^{cc,ap}(i\omega)$, and this last GF can be used to express the other GF's in a more compact way. In the computational calculation we fix the chemical potential at $\mu = 0$, we vary the conduction atomic level ε_o in such a way that the Friedel sum rule³² should be satisfied¹⁰

$$\rho_{f\sigma}(\mu) = \frac{\sin^2(\pi n_{f\sigma})}{\Delta\pi}, \quad (60)$$

where $n_{f,\sigma}$ is the occupation number of the localized states and $\rho_{f,\sigma}(\mu)$ is the f-electron density of states at the chemical potential. We then fix the parameter \tilde{V} so that the Kondo temperature is given by Eq. (59); this procedure guarantees two important characteristics of the Kondo resonance: the correct height of the Kondo peak, obtained by the imposition of the Friedel sum rule, and the correct width given by the Kondo temperature, obtained through the choice of \tilde{V} .

In the exact GF all the energies $E_{\mathbf{k},\sigma}$ of the conduction band contribute to the exact effective cumulant $M_\sigma^{eff}(z)$, but only the single energy ε_o of the atomic level appears in the $M_\sigma^{ap}(z)$ of the approximate GF. The advantage of the atomic approximation is that it seems reasonable to expect that it would give a good description of the problem.

X. RESULTS FOR THE SINGLE IMPURITY ANDERSON MODEL (SIAM)

One can use our atomic approach to describe a large number of nanoscopic systems, as well as macroscopic Kondo systems like intermediate valence ones or other heavy fermion systems. The Eq. (38) for the atomic case can be diagonalized exactly, and in Fig. 1 we show the eigenenergies and transitions for a particular case that corresponds to the Kondo regime, with values $U = 18\Delta$, E_f

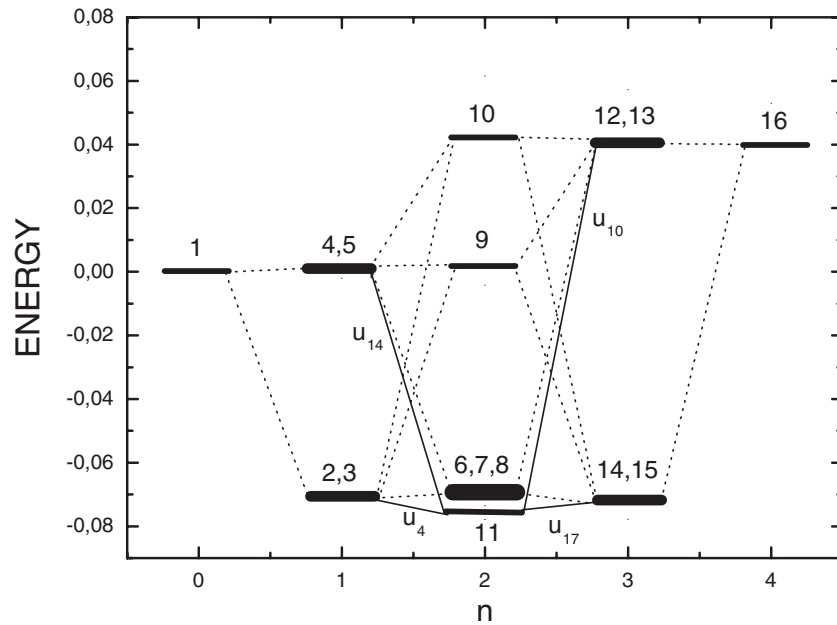


FIG. 1. Plot of the 16 eigenstates of the atomic Anderson model for a band with zeroth width, for $U = 18.0\Delta$, $E_f = -7.0\Delta$, and $T = 0.001\Delta$. The allowed transitions that are used to calculate the GF are shown, employing bold lines for those that give the peaks of the density of states of Fig. 2.

$= -7.0\Delta$, $T = 0.001\Delta$, and $\mu = 0$, where $\Delta = \pi V^2/2D = 0.01D$ and $D = 1.0$. The ground state of this system is a two-particle singlet with energy E_{11} , and just above this state there is a triplet with energies E_6, E_7, E_8 . This figure shows with bold lines the transitions that correspond to the f -electron density of states plotted in Fig. 2: the lower band is associated to the transition (u_{14}), the upper band to the transition (u_{10}) and the Kondo peak to the transitions (u_4, u_{17}) that originate the resonance structure around the chemical potential μ . In that figure we show the spectral densities for the following values of the f -electron positions: $E_f = -2.0\Delta$, $E_f = -5.0\Delta$, and $E_f = -9.0\Delta$, when $T = 0.001\Delta$ and $U = 18.0\Delta$. The symmetric case with $|E_f| = U/2$ is given by $E_f = -9.0\Delta$, and the $E_f = -2.0\Delta$ enters into the intermediate valence regime at larger T . In the inset of the figure it is shown how the Kondo peak width changes exponentially with E_f from close to the intermediate valence regime ($E_f = -2.0\Delta$) into the Kondo one ($E_f = -5.0\Delta$) and the extreme Kondo limit (the symmetric case at $E_f = -9.0\Delta$). When E_f changes, the Kondo peak remains at the chemical potential, and its width follows the Kondo temperature according to Eq. (59).

XI. CONDUCTANCE FOR THE SINGLE ELECTRON TRANSISTOR (SET)

We shall study here the electronic conduction through a quantum dot (QD) embedded in a quantum wire (QW), which is realized experimentally in a single electron transistor (SET). It was theoretically predicted^{33,34} that a Kondo singlet should form in a single-electron transistor (SET), which contains a confined “droplet” of electrons coupled by quantum-mechanical tunneling to the delocalized electrons in the transistor’s leads. The number of electrons at the quantum dot can change from zero up to a maximum of two by changing the chemical potential μ . In an earlier paper³⁵ we applied the X –boson approach for $U \rightarrow \infty$ to calculate the conductance of a QD side coupled to the leads, and here we calculate the conductance of a SET for the finite U case. This system was experimentally studied by the Goldhaber-Gordon group,^{5,6} and recently appeared a complete numerical renormalization group (NRG) calculation which should be compared with our results.²⁷ In Fig. 3 we present a schematic view of the quantum dot embedded in a quantum wire, here described by a ballistic channel. With small bias voltage and low temperature the electronic transport is coherent, and when a linear response calculation is employed,³⁶ an expression of the

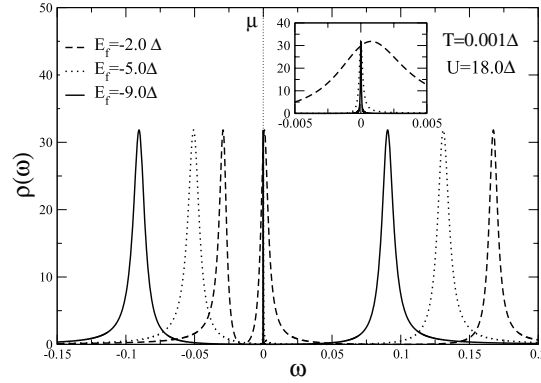


FIG. 2. Density of states of the single impurity Anderson model (SIAM) in the atomic approach, for $T = 0.001\Delta$, $U = 18.0\Delta$ and in the Kondo regime, from very close to the intermediate valence regime ($E_f = -2.0\Delta$) to well inside the Kondo region ($E_f = -5.0\Delta$ and $E_f = -9.0\Delta$). The last plot corresponds to the symmetric case with $|E_f| = U/2$. In the inset we represent a detail of the Kondo peak corresponding to different values of E_f .

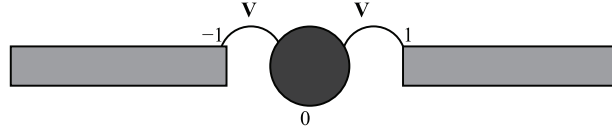


FIG. 3. Schematic picture of a quantum dot embedded to a conduction leads. This system is realized experimentally in a single electron transistor (SET).

Landauer type is obtained for the conductance:

$$G = \frac{2e^2}{h} \int \left(-\frac{\partial n_f}{\partial \omega} \right) S(\omega) d\omega. \quad (61)$$

Here n_f is the Fermi function, and

$$S(\omega) = \Gamma^2 |\tilde{G}_0^\sigma|^2 \quad (62)$$

is the probability of transmission of an electron with energy $\hbar\omega$, where the strength of the coupling between the QD and the wire is Γ . Employing the GF $G_\sigma^{ff}(\omega)$ of the f-electrons at the QD as well as the GF $G_c^\sigma(\omega)$ of the leads, described here as a ballistic channel, we can write as follows the dressed GF $\tilde{G}_0^\sigma(\omega)$ at the QD:

$$\tilde{G}_0^\sigma(\omega) = G_c^\sigma(\omega)^2 V^2 G_\sigma^{ff}(\omega). \quad (63)$$

In this equation we use our approximate GF $G_\sigma^{ff}(\omega)$, discussed in Section IX (cf. Eqs. (26) and (27) of Ref. (10) together with our Eqs. (55)–(58)), as well as $G_c^\sigma(\omega) = -(1/2D) \ln [(\omega + D)/(\omega - D)]$ (where $\omega \Rightarrow \omega + i\eta$, with $\eta \rightarrow 0^+$).

In Fig. 4 we show the conductance as a function of E_f , obtained with the parameters used in Sec. X in Figs 1 and 2, namely $U = 18\Delta$ and $T = 0.001\Delta$, and the figure shows four important regions. In the empty-dot region the level E_f is above the chemical potential, so that the f-electron occupation vanishes ($n_f \rightarrow 0$) together with the conductance: $G/G_0 \rightarrow 0$, where the constant $G_0 = 2e^2/h$ is the maximum conductance in the ballistic limit. In this region there is no Kondo peak, and the electrons can not jump thorough the quantum dot. Decreasing E_f the intermediate valence region appears (“IV region” in the graph) and E_f is close to the chemical potential $\mu = 0$. There are strong charge fluctuations in this regime, the Kondo resonance starts to appear at the chemical potential μ and the conductance G increases rapidly with decreasing E_f , until the Kondo region appears when the embedded QD goes into the Kondo regime. In this region the occupation number is close to one ($n_f \simeq 1$), the Kondo peak is formed and the conductance reaches its maximum value: $G/G_0 \rightarrow 1$ because there is a perfect transmission through the Kondo resonance at the chemical potential. In the

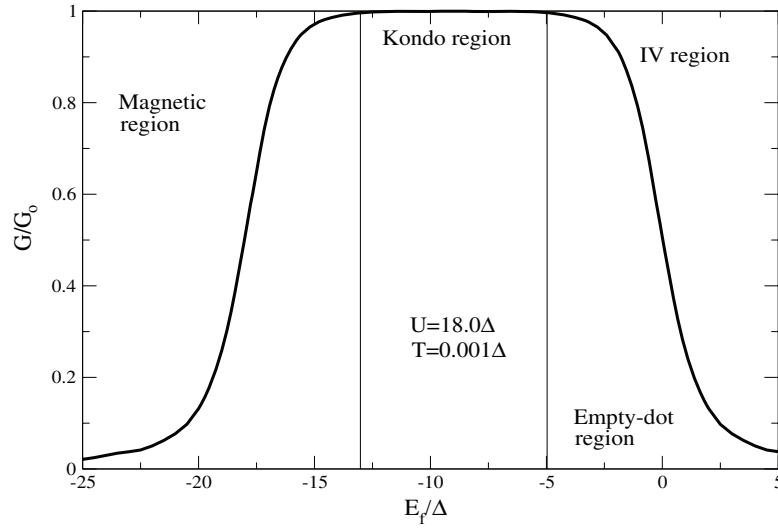


FIG. 4. Normalized conductance of the embedded quantum dot for $U = 18.0\Delta$ and $T = 0.001\Delta$.

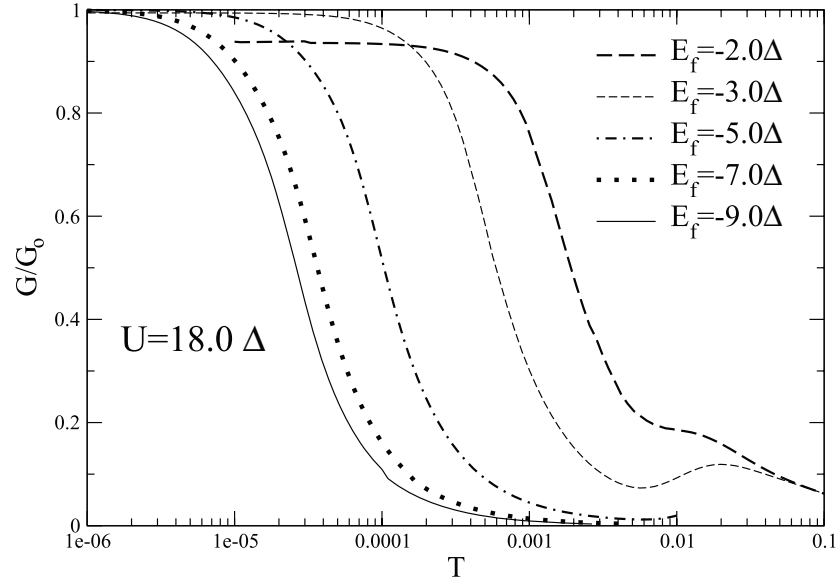


FIG. 5. Behavior of the conductance for $U = 18.0\Delta$ as a function of temperature for different values of the localized levels E_f . As E_f approaches the symmetric limit of the model, the Kondo temperature varies exponentially and the conductance displaces to lower temperatures values.

fourth region we have $n_f > 1$, and the regime is dominated by the double occupation (cf. Ref. 10). We call this region “magnetic”, and when E_f decreases further we have $n_f \rightarrow 2$ and the conductance goes to zero because of the disappearance of the Kondo resonance. We used our atomic approach to calculate the conductance G , and in Fig. 5 we plot the temperature dependence of G/G_0 for several values of E_f ($G_0 = 2e^2/h$ is the ballistic channel conductance). The different localized E_f values we employ ($E_f = (-2.0; -3.0; -5.0; -7.0; -9.0)\Delta$) correspond respectively to Kondo temperatures $T_K = (0.001838; 0.0005911; 0.0001032; 0.00003621; 0.00002553)$ that satisfy Eq. (59). This is achieved by employing the universality of G/G_0 as a function of T/T_K to find the \tilde{V} that gives this result when calculated with the GF in the atomic approach (see below), and these values guarantee that the Kondo peak at the chemical potential μ has the correct width. The values of \tilde{V} corresponding to the E_f above are respectively: $\tilde{V} = (0.008565; 0.00546; 0.00294; 0.001992; 0.001757)$. It is interesting to

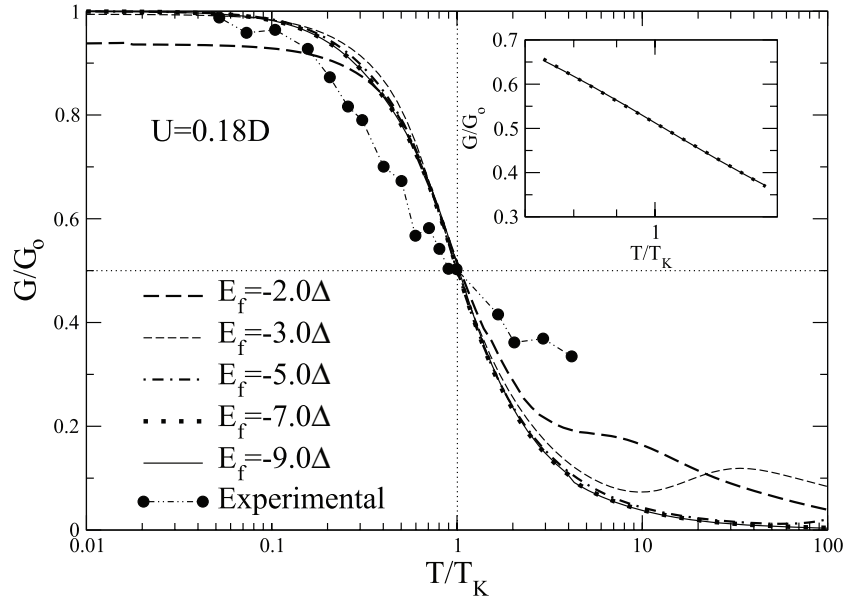


FIG. 6. Universal behavior of the conductance for $U = 18.0\Delta$ in the Kondo region for the same parameters of Fig. 5. In the inset we show the logarithmic dependence of G/G_o close to T_K : the full curve corresponds to the symmetric case and the points correspond to the linear fit to a logarithmic curve.

observe that the $\tilde{V} = 0.008565$ corresponding to the $E_f = -2.0\Delta$ is close to the Anderson parameter $\Delta = 0.01$ employed in our earlier works^{9,10} as well as in Costi's NRG calculations.³⁷ One important characteristic of the conductance is its universality in the Kondo regime, as first pointed out by Costi *et al.*²⁶ which showed that the transport coefficients for the particle-hole symmetric Anderson model are universal. In a seminal work in 1998, Goldhaber-Gordon *et al.*⁵ measured the conductance of a SET and showed its universal character. Recently M. Yoshida *et al.*²⁷ employing a NRG, have shown that the conductance of the SET is also universal in the Kondo regime in the asymmetric case, taking the form

$$\tilde{G}(T/T_K) - \frac{G_o}{2} = - \left(\tilde{G}^S(T/T_K) - \frac{G_o}{2} \right) \cos(\pi n_f) \quad (64)$$

where $\tilde{G}(T/T_K) = G(T)$, $\tilde{G}^S(T/T_K)$ corresponds to the symmetric case, and we have substituted by πn_f the phase shifts that appear in their expression (cf. Eq. (49) in Ref. 27). When $n_f = 1$ we obtain $\tilde{G}(T/T_K) = \tilde{G}^S(T/T_K)$, so that well into the Kondo region ($n_f = 1$) we recover the universality of the symmetric model. The T_K has been defined in the symmetric model²⁷ through $G^S(T_K) = G_o/2$, and it then follows from Eq. (64) that for the asymmetric case $G(T_K) = G_o/2$ is also valid. That relation has been already employed to extract T_K both from the experimental values⁵ of $G(T)$ and from the calculations with the NRG.²⁷ As discussed above, we use this relation to extract the T_K from the values of $G(T)$ calculated with the atomic approach, and vary the \tilde{V} so that T_K coincides with the corresponding value given in Eq. (59). By this method we calculated the normalized conductance G/G_o as a function of the T/T_K for several values of the localized level $E_f = (-2.0; -3.0; -5.0; -7.0; -9.0)\Delta$, and we plot them in Fig. 6. It is interesting to give their occupation numbers n_f at low T : they are $n_f = (0.84032237, 0.94162564, 0.99067072, 0.99853634, 1.00046049)$ and from Eq. (64) it is clear why the last four curves practically collapse at low T , while the first one starts below $G/G_o = 1.0$. At low T these curves are in the Kondo region, while for $E_f = 0$, with $n_f = 0.50345512$, the system is in the intermediate valence region. The points in Fig. 6 represent the experimental results extracted from the Goldhaber-Gordon measurements⁵ (Reprinted data extracted from Figs. 3 and 4 with permission from D. Goldhaber-Gordon, J. Göres, M. A. Kastner, Hadas Shtrikman, D. Mahalu, and U. Meirav, Physical Review Letters, vol. 81, page 5225, year 1998. Copyright 1998 by the American Physical Society. <http://link.aps.org/doi/10.1103/PhysRevLett.81.5225>). The atomic

approach results agree better with them for $T/T_K < 1$, but for $T/T_K > 1$ the results are not so good; this is a consequence of the use in the atomic approach of the Friedel sum rule, which is exact only at $T = 0$. It should be pointed out that the atomic approach produces results comparable to the experimental ones for low temperatures, but from our point of view, it does not substitute the NRG results that are very close to the experimental ones.⁵

XII. CONCLUSIONS

In our previous papers^{9,10} we developed the atomic approach in the limit of infinite and finite correlation U , and suggested that it was an alternative to study nanoscopic systems that exhibit the Kondo effect. Due to the simplicity of its implementation and the very low computational cost, the atomic approach is a good candidate to describe strongly correlated atomic impurities or lattice systems that exhibit the Kondo effect. In this work we calculate approximate Green's Functions of the single impurity Anderson model (SIAM), by starting from a formally exact expression of the GF, and substituting a component of this expression by the one corresponding to the exact solution of the atomic Anderson problem (AAS). We call this technique the atomic approach, not to be confused with the atomic solution of the Anderson limit.³⁸ The densities of states obtained with the method present a Kondo peak that has a correct height⁹ $1/\pi \Delta$ and exhibit the correct exponential variation of the Kondo temperature.²⁸ We calculate several density of states representative of the Kondo regime for finite correlation U , including the symmetrical case, in the single impurity Anderson model (SIAM). We have also calculated the conductance of a single electron transistor (SET) in the finite U case for the different regimes of the system, and we obtain a good agreement with available experimental results^{5,6} as well as with theoretical ones that employ the NRG.²⁷

ACKNOWLEDGMENTS

We would like to express our gratitude to the Conselho Nacional de Desenvolvimento Científico (CNPq) - Brazil.

- ¹ J. Kondo, *Progress of Theoretical Physics* **32**, 37 (1964).
- ² M. Garnier, K. Breuer, D. Purdie, M. Hengsberger, Y. Baer, and B. Delley, *Phys. Rev. Lett.* **78**, 4127 (1997).
- ³ J. Li, W.-D. Schneider, R. Berndt, and B. Delley, *Phys. Rev. Lett.* **80**, 2893 (1998).
- ⁴ V. Madhavan, W. Chen, T. Jamneala, M. F. Crommie, and N. S. Wingreen, *Phys. Rev. B*, 165412 (2001).
- ⁵ Goldhaber-Gordon, J. Gores, M. A. Kastner, H. Shtrikman, D. Mahalu, and U. Meirav, *Phys. Rev. Lett.* **81**, 5225 (1998).
- ⁶ D. Goldhaber-Gordon, H. Shtrikman, D. Mahalu, D. Abusch-Magder, U. Meirav[†], and M. A. Kastner, *Nature* **391**, 156 (1998).
- ⁷ M. S. Figueira, M. E. Foglio, and G. G. Martinez, *Phys. Rev. B* **50**, 17933 (1994).
- ⁸ C. Noce, *Physics Reports* **431**, 173 (2006).
- ⁹ T. Lobo, M. S. Figueira, and E. Foglio, *Nanotechnology* **17**, 6016 (2006).
- ¹⁰ T. Lobo, M. S. Figueira, and M. E. Foglio, *Nanotechnology* **21**, 274007 (2010).
- ¹¹ The main purpose of the present paper is to summarize the derivation of the approximate GF in the atomic approach, and most of its lengthy details are included in an electronic archive deposited at the Los Alamos electronic repository¹³ (we shall use **II** to indicate this reference). Other details not given in the present paper, like the analytic solution of the AAS, can be found in Ref. 10.
- ¹² When we write Eq. (2) employing $X_{0\sigma}$ and $X_{\bar{\sigma}d}$ it appears $\sigma X_{\bar{\sigma}d}$ rather than $X_{\bar{\sigma}d}$. We then have to write the $V_{j,ba,\mathbf{k},\sigma}$ in Eq. (14) in the following way: $V_{j,\bar{\sigma}d,\mathbf{k},\sigma} = \sigma V_{j,0\sigma,\mathbf{k},\sigma} = \sigma V_{j,\mathbf{k},\sigma}$.
- ¹³ M. E. Foglio, T. Lobo, and M. S. Figueira, "Green's functions for the Anderson model: The atomic approximation," (2010), arXiv:0903.0139 [cond-mat].
- ¹⁴ M. Wortis, *Phase Transitions and Critical Phenomena*, edited by C. Domb, and M. S. Green, Vol. 3 (Academic, London, 1974) p. 113.
- ¹⁵ J. Hubbard, *Proc. R. Soc. London, Ser. A* **296**, 82 (1967).
- ¹⁶ In that Appendix, the $v(\alpha, \mathbf{k}, \sigma, \pm u)$ in the item 2(b) of **Rule C.2** should be changed into $V(\alpha, \mathbf{k}, \sigma, \pm u)$.
- ¹⁷ A factor $(-1)^n$ appears also in the perturbation expansion contribution of any graph of order n , i.e. with n internal edges (cf. the cumulant expansion for the Ising model in Ref. 14, where this sign has been included in the interaction constant in its Eq. (2)). We have then added a factor (-1) to every internal edge, and therefore this extra factors would only change the sign of a graph's contribution when it is of odd order. This sign appears explicitly in the expansion of the PAM in **I** (cf. Eqs. (3.8) and (3.11) of that reference) but it was left out from the diagrams contribution by an oversight. Note that this sign does not depend on the Fermionic character of the X operators.

- ¹⁸ To simplify the notation we use $\Delta(x) = 0$ when $x \neq 0$ and $\Delta(0) = 1$.
- ¹⁹ A. L. Fetter and J. D. Walecka, *Quantum Theory of Many-Particle Systems* (McGraw-Hill, New York, 1971).
- ²⁰ J. M. Luttinger and J. C. Ward, *Phys. Rev.* **118**, 1417 (1960).
- ²¹ W. Metzner, *Phys. Rev. B* **43**, 8549 (1991).
- ²² L. Craco and M. A. Gusmão, *Phys. Rev. B* **54**, 1629 (1996).
- ²³ M. E. Foglio and M. S. Figueira, *J. Phys. A Mathematics and General* **30**, 7879 (1997).
- ²⁴ M. E. Foglio, *Brazilian Journal of Physics* **27**, 644 (1997).
- ²⁵ M. E. Foglio and L. M. Falicov, *Phys. Rev. B* **20**, 4554 (1979).
- ²⁶ A. Costi, A. C. Hewson, and V. Zlatić, *J. Phys.: Condens. Matter* **6**, 2519 (1994).
- ²⁷ M. Yoshida, A. C. Seridonio, and L. N. Oliveira, *Phys. Rev. B* **80**, 235317 (2009).
- ²⁸ A. C. Hewson, *The Kondo Problem to Heavy Fermions* (Cambridge University Press, 1993).
- ²⁹ A. S. da Rosa Simões, J. R. Iglesias, A. Rojo, and B. R. Alascio, *J. Phys. C: Solid State Phys.* **21**, 1941 (1988).
- ³⁰ C. Noce, *J. Phys.: Condens. Matter* **3**, 7819 (1991).
- ³¹ M. Marinaro, C. Noce, and A. Romano, *J. Phys.: Condens. Matter* **3**, 3719 (1991).
- ³² D. C. Langreth, *Phys. Rev.* **150**, 516 (1966).
- ³³ T. K. Ng and P. A. Lee, *Phys. Rev. Lett.* **61**, 1768 (1988).
- ³⁴ L. I. Glazman and M. E. Raikh, *JETP Lett.* **47**, 452 (1988).
- ³⁵ R. Franco, M. S. Figueira, and E. V. Anda, *Phys. Rev. B* **67**, 155301 (2003).
- ³⁶ K. Kang, S. Y. Cho, J. J. Kim, and S. C. Shin, *Phys. Rev. B* **63**, 113304 (2001).
- ³⁷ T. A. Costi, J. Kroha, and P. Wolfle, *Phys. Rev. B* **53**, 1850 (1996).
- ³⁸ We should also stress that the atomic approach can be easily extended to study the Anderson lattice (cf. **II**). In this case, we first solve the impurity problem satisfying the Friedel sum rule to obtain the approximate cumulants M_{σ}^{ap} , and employing these approximate cumulants we calculate the lattice Green's functions. This opens the possibility of applying the method to a broad class of physical problems governed by the Kondo scale: quantum dots, Anderson impurity problems, Kondo insulators and intermediate and heavy fermion problems.